Regular Article - Theoretical Physics

Viscous effect in the late time evolution of phantom universe

Jing Yang, Rui-Hui Lin[a] , **Chao-Jun Feng**[b] , **Xiang-Hua Zhai**[c]

Division of Mathematics and Theoretical Physics, Shanghai Normal University, 100 Guilin Road, Shanghai 200234, China

Abstract We investigate the cosmological implications of a phantom dark energy model with bulk viscosity. We explore this model as a possible way to resolve the big rip singularity problem that plagues the phantom models. We use the latest type Ia supernova and Hubble parameter data to constrain the model parameters and find that the data favor a significant bulk viscosity over a non-constant potential term for the phantom field. We perform a dynamical analysis of the model and show that the only stable and physical attractor corresponds to a phantom-dominated era with a total equation of state that can be greater than -1 due to the viscosity. We also study the general effect of viscosity on the phantom field and the late time evolution of the universe. We apply the statefinder diagnostic to the model and find that it approaches a nearby fixed point asymptotically, indicating that the universe can escape the big rip singularity with the presence of bulk viscosity. We conclude that bulk viscosity can play an important role in affecting the late-time behavior as well as alleviating the singularity problem of the phantom universe.

1 Introduction

Cosmological observations in recent decades have revealed more details about the evolutional history of the universe. One of the major discoveries is the late time acceleration of cosmic expansion, which can be generally understood from at least two different perspectives. Either Einstein's theory of gravity is incomplete and calls for modifications (for recent reviews, see, e.g., Refs. [1,2]), or there is an unknown form of energy dubbed dark energy (DE) that exhibits repulsive behavior. The simplest model of DE is the cosmological constant Λ model with cold dark matter (ΛCDM), which

assumes that DE consists of a constant energy density that fills the space uniformly and has a constant equation of state (EoS) $w_{DE} = -1$, where w_{DE} is the ratio of pressure to energy density of the DE content.

However, the cosmological constant has no clear physical origin and faces several theoretical challenges (see, e.g., Ref. [3]). Therefore, many alternative DE models have been proposed and explored (see, e.g., Refs. [4–6]). These models can be roughly divided into two categories: the quintessence model with $w_{DE} > -1$ [7,8] and the phantom model with $w_{DE} < -1$ [9,10], which have different implications for the ultimate fate of the universe. Quintessence models generally predict that the universe will undergo an eternal expansion, while phantom models usually indicate that the universe will enter a super-accelerated expansion phase and end in a finite time with a cosmic singularity known as big rip, where all structures will be torn apart. Recent observations seem to favor the phantom model over the quintessence model [9,11–14]. Nonetheless, such discussions about w_{DE} rest upon the assumption that it is simply given by p_{DE}/ρ_{DE}. This representation is purely phenomenological and lacks underlying physics. To provide a more comprehensive understanding of the nature of DE including its temporal evolution or perturbation, a more fundamental framework should be considered. One approach involves introducing a dynamic scalar field as part of either the quintessence or phantom models, depending on the specific properties of its potential and kinetic terms [9]. In particular, the phantom scalar field model has attracted significant interests within the literature (see, e.g., Refs. [4,13,15] and the references therein).

The studies of phantom models typically lead to discussions about the big rip singularity [16–25]. To address this issue, researchers have introduced modifications to DE based on quantum effects [26], geometric effects derived from modified gravities [27,28], or interactions between cosmic content [29,30]. One way to introduce interactions involves considering the viscosity of each component. This approach

[a] e-mail: linrh@shnu.edu.cn (corresponding author)

[b] e-mail: fengcj@shnu.edu.cn

[c] e-mail: zhaixh@shnu.edu.cn

accounts for the dissipative properties of real fluids. In particular, bulk viscosity is the most relevant for cosmology since we assume a homogenous and isotropic universe. This can be incorporated into the standard cosmological scheme by redefining the effective pressure $p_{\text{eff}} = p - \Pi$ with a viscous pressure term Π to restore thermal equilibrium [31–33].

Invoking viscosity in cosmology is proven to be useful to resolve or soften the cosmic singularity problem in different models [34–41]. Following this approach, it is shown that the singularity problem can be alleviated in the anisotropic phantom universe with viscosity [25]. Moreover, an interacting phantom DE with dark matter induced by the viscous approach is shown to be able to avoid the big rip singularity [17,18].

In this work, we will study viscous phantom scalar field DE model and explore its late time behavior. The paper is structured as follows. In Sect. 2, we review the phantom scalar field model of DE and introduce the viscous cosmology framework. Section 3 contains the late time observation fit to constrain the model parameters. Dynamical system analysis and statefinder diagnostic of the model are given in Sects. 4 and 5, respectively. And we conclude our study in the last section.

2 Viscous phantom scalar field DE model

The action for a phantom field minimally coupled to gravity is given by

$$S = \int d^4x \sqrt{-g} \left[-(\partial\phi)^2 + V(\phi) \right], \tag{1}$$

where $V(\phi)$ is the potential of the phantom field ϕ. The energy density and pressure of the phantom field are [9]

$$\begin{aligned} \rho_\phi &= -\frac{1}{2}\dot{\phi}^2 + V(\phi), \\ p_\phi &= -\frac{1}{2}\dot{\phi}^2 - V(\phi). \end{aligned} \tag{2}$$

We assume a spatially flat*** Friedmann-Lemaître-Robertson-Walker metric for the homogeneous and isotropic universe, given by

$$ds^2 = dt^2 - a(t)^2 \left[dr^2 + r^2 \left(d\theta^2 + \sin^2\theta d\psi^2 \right) \right], \tag{3}$$

where $a(t)$ is the scale factor. Then, the Friedmann equations read

$$\begin{aligned} H^2 &= \frac{1}{3}\left(\rho_m + \rho_\phi \right), \\ \dot{H} &= -\frac{1}{2}\left(\rho_m + \rho_\phi + p_\phi \right), \end{aligned} \tag{4}$$

where ρ_m and p_m are the energy density and pressure of dust matter, respectively, $H = \frac{\dot{a}}{a}$ is the Hubble parameter, and the dot represents the derivative with respect to the cosmic time t.

As mentioned in the Introduction, the bulk viscosity dissipation in the cosmic phantom field fluid can be represented by a pressure term $-\Pi$ added to p_ϕ. For bulk viscosity related to the cosmic expansion, we assume that $\Pi \propto H$, which implies that the effective pressure of the phantom field is

$$p_{\text{eff}} = p_\phi - 3\xi_\phi H, \tag{5}$$

where ξ_ϕ is the viscosity coefficient. Then, the evolutionary equations for dust matter and the phantom field are given by

$$\begin{aligned} \dot{\rho}_m + 3H\rho_m &= 0, \\ \dot{\rho}_\phi + 3H(\rho_\phi + p_\phi - 3H\xi_\phi) &= 0. \end{aligned} \tag{6}$$

Using Eq. (2), we obtain the equation for the phantom field

$$\ddot{\phi} + 3H\dot{\phi} - V'(\phi) + \frac{9\xi_\phi H^2}{\dot{\phi}} = 0, \tag{7}$$

where the prime denotes the derivative of the potential V with respect to the field ϕ.

Generally, the viscosity of a fluid may depend on energy density, pressure, spacetime geometry and so on. For simplicity, in the current work, we assume the viscosity is proportional to the changing rate of the phantom field, i.e.,

$$\xi_\phi = \xi_0\dot{\phi}, \tag{8}$$

where the viscosity coefficient ξ_0 is a constant parameter. As for the potential of the phantom field, it is shown that an exponential form of potential can match or account for the acceleration of expansion [42–47], which is then adopted in the current work and is given by

$$V(\phi) = V_0 e^{-\alpha_0\phi}, \tag{9}$$

where α_0 and V_0 are constants.

3 Observational constraints

We constrain the viscous phantom model using the late-time observational data sets based on Markov Chain Monte Carlo method. We use the Pantheon compilation of Type Ia supernova (SNIa) [5] and Hubble parameter ($H(z)$) data points [48] to fit the model parameters. The SNIa data consist of 279 samples from Sloan Digital Sky Survey (SDSS) and Supernova Legacy Survey (SNLS) with redshifts $0.03 < z < 0.68$, and 1048 samples with redshifts $0.01 < z < 2.3$ including the Hubble Space Telescope (HST) samples and various low-z samples. The $H(z)$ data include 26 data points from Baryon

Table 1 The best fitting values of model parameters and 1σ confidence level for Model P and Model vP under Pantheon+H(z) data sets

Parameter	Model P	Model vP
Ω_m	$0.331^{+0.026}_{-0.025}$	$0.322^{+0.003}_{-0.003}$
H_0	$68.31^{+1.16}_{-1.14}$	$68.31^{+1.23}_{-1.20}$
V_0/H_0^2	$2.184^{+0.102}_{-0.087}$	$2.612^{+0.347}_{-0.261}$
α_0	$1.262^{+0.479}_{-0.436}$	$-0.04^{+0.355}_{-0.309}$
ξ_0	–	$0.323^{+0.099}_{-0.106}$
χ^2_{min}/dof	$1053.93/1099$	$1053.174/1098$

Acoustic Oscillations and 31 data points from the differential age method. For comparison, besides fitting the viscous phantom model under consideration (denoted as Model vP in the following), we also perform the same fitting procedure for the phantom model without viscosity (denoted as Model

P in the following). The fitting results are summarized in Table 1.[1] Figure 1 shows the constraints on the parameters of Model vP at 2σ confidence level.

One can see that for Model P, the phantom potential cannot be constant at 1σ confidence level as the phantom field is the sole mechanism in operation for the late-time cosmic acceleration. However, if both the viscosity and the phantom field with its potential are taken into consideration, as in Model vP, the fitting result favors a significant viscosity and does not exclude the constant potential case with $\alpha_0 = 0$.

4 Dynamical analysis

By using the dimensionless variables [42,43,51]

$$x = \frac{\dot{\phi}}{\sqrt{6}H}, \quad y = \frac{\sqrt{V(\phi)}}{\sqrt{3}H},$$
$$\zeta = \frac{\xi_\phi}{H} = \xi_0 \frac{\dot{\phi}}{H} = \sqrt{6}\xi_0 x, \tag{10}$$

the partial differential equations of the phantom scalar field can be recast into an autonomous system as

$$\frac{dx}{dN} = -3x - \frac{\sqrt{6}}{2}\alpha_0 y^2 + \frac{3}{2}x\left[1 - x^2 - y^2 - \sqrt{6}\xi_0 x\right]$$
$$- \frac{3\sqrt{6}}{2}\xi_0, \tag{11}$$
$$\frac{dy}{dN} = -\frac{\sqrt{6}}{2}\alpha_0 xy + \frac{3}{2}y\left[1 - x^2 - y^2 - \sqrt{6}\xi_0 x\right],$$

where $N = \ln a = -\ln(1 + z)$. The Friedmann equation can also be rewritten as a dimensionless constraint

$$\Omega_m + \Omega_\phi = \Omega_m - x^2 + y^2 = 1, \tag{12}$$

where $\Omega_i = \frac{\rho_i}{3H^2}$ is the density parameter of the corresponding component.

The critical points of the above system and their existence conditions are listed in Table 2.

The stability of each critical point can be inferred from the eigenvalues of the linearized perturbation matrix $\mathcal{M}$ of the autonomous given by

$$\mathcal{M} = \begin{pmatrix} -\frac{3}{2}\left(1 + 3x^2 + y^2 + 2\sqrt{6}\xi_0 x\right) & -3xy - \sqrt{6}\alpha_0 y \\ -3xy - \sqrt{6}\alpha_0 y - \frac{3\sqrt{6}}{2}\xi_0 y & -\frac{1}{2}\left(3 + 3x^2 + 9y^2 + \sqrt{6}\alpha_0 x + \frac{3\sqrt{6}}{2}\xi_0 x\right) \end{pmatrix}. \tag{13}$$

- **For critical point A_1**, the eigenvalues of the linearized perturbation matrix are

$$\eta^{(1)}_{A_1} = -\frac{3C_1 + C_2}{4\alpha_0^4},$$
$$\eta^{(2)}_{A_1} = -\frac{3C_1 - C_2}{4\alpha_0^4}, \tag{14}$$

where
$$C_1 = \alpha_0^4 - 3\alpha_0^3\xi_0,$$
$$C_2 = \sqrt{-6\alpha_0^6\left[24 + 78\alpha_0\xi_0 + 16\alpha_0^3\xi_0 - 9\xi_0^2 + \alpha_0^2(7 + 48\xi_0^2)\right]}. \tag{15}$$

In Fig. 2, the colored areas mark the possible regions of parameters for the critical point A_1 to exist. The stable (pink) and saddle (blue) regions are divided by the line $\Omega_\phi = 1$. However, the conditions $0 \le \Omega_m, \Omega_\phi \le 1$ further rule out the unphysical regions (shaded) of the parameters ξ_0 and α_0.

- **For critical point A_2**, the eigenvalues of the linearized perturbation matrix are

$$\eta^{(1)}_{A_2} = \frac{3}{2} + 3\alpha_0\xi_0,$$
$$\eta^{(2)}_{A_2} = -\frac{3}{2} - 9\xi_0^2. \tag{16}$$

Fig. 1 Constraints on the viscous phantom model parameters from 1σ to 2σ confidence level. Where $\gamma = V_0/H_0^2$
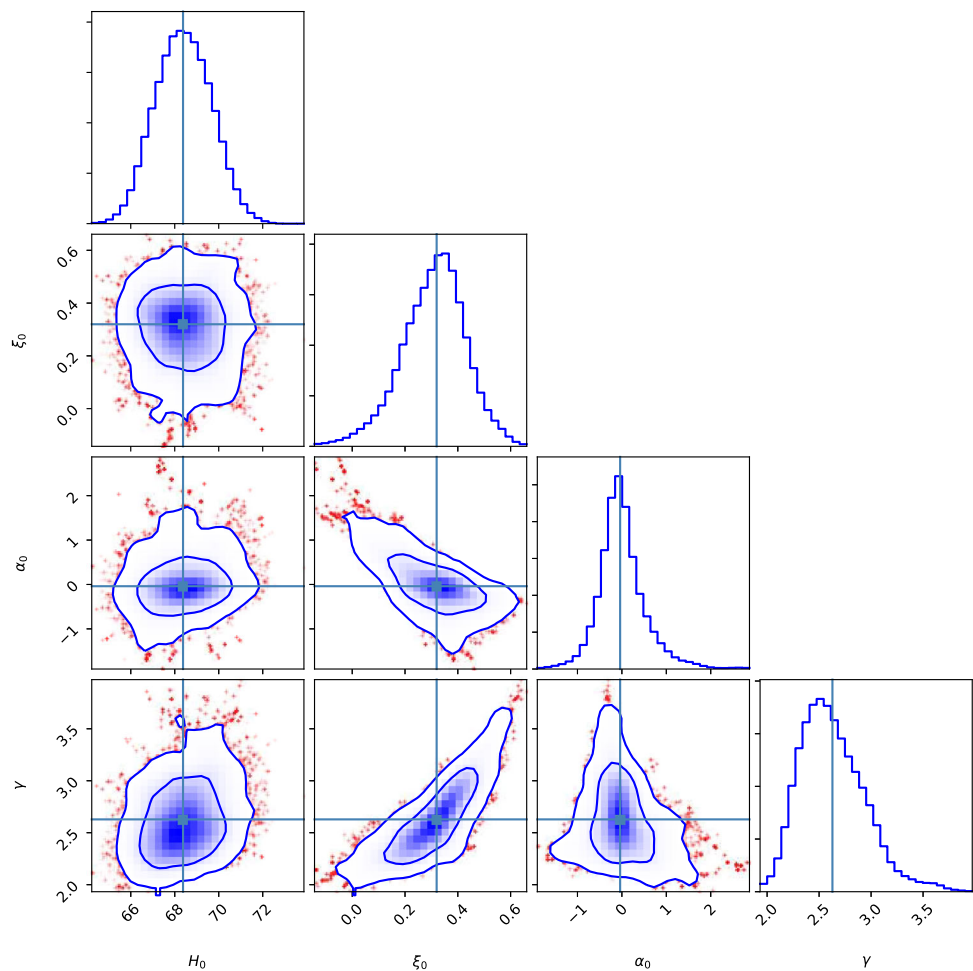

Table 2 The critical points and their existence conditions of autonomous system (11)

| Critical points	(x, y)	Existence conditions	Ω_ϕ
A_1	$\left(\dfrac{\sqrt{\frac{3}{2}}}{\alpha_0}, \dfrac{\sqrt{-\frac{3}{2}-3\alpha_0\xi_0}}{\alpha_0}\right)$	$\left(\xi_0 < 0 \text{ and } \alpha_0 > -\frac{1}{2\xi_0}\right)$ or $\left(\xi_0 > 0 \text{ and } \alpha_0 < -\frac{1}{2\xi_0}\right)$	$-\dfrac{3(1+\alpha_0\xi_0)}{\alpha_0^2}$
A_2	$(-\sqrt{6}\xi_0, 0)$	All ξ_0 and $\alpha_0 \neq 0$	$-6\xi_0^2$
A_3	$\left(-\dfrac{\alpha_0+3\xi_0}{\sqrt{6}}, \dfrac{\sqrt{6+(\alpha_0+3\xi_0)^2}}{\sqrt{6}}\right)$	All ξ_0 and $\alpha_0 \neq 0$	1

A_2 exists as long as $\alpha_0 \neq 0$. The sign of the first eigenvalue $\eta_{A_2}^{(1)}$ is bifurcated by the hyperbola $\alpha_0\xi_0 = -1/2$, while the second eigenvalue $\eta_{A_2}^{(2)}$ is always negative for any real value of parameter ξ_0. Therefore, the stable (pink) and saddle (blue) regions of A_2 are shown as Fig. 3. However, we note that A_2 only exists when $\Omega_\phi < 0$. This scenario is also known as the perfect fluid supra-dominated era [52], which is beyond the scope of the current work and is considered unphysical. We constrain the parameters α_0 and ξ_0 as such that $0 \leq \Omega_m, \Omega_\phi \leq 1$ and this point A_2 will not exist.

- **For critical point** A_3, the eigenvalues of the linearized perturbation matrix are

$$\eta_{A_3}^{(1)} = -3 - \alpha_0(\alpha_0 + 3\xi_0),$$
$$\eta_{A_3}^{(2)} = -\frac{1}{2}(6 + (\alpha_0 + 3\xi_0)^2). \tag{17}$$

A_3 also exists for $\alpha_0 \neq 0$ and any real ξ_0. The second eigenvalue $\eta_{A_3}^{(2)}$ is always negative, while the first one can have either sign. The stable (pink) and saddle (blue) regions of A_3 are shown in Fig. 4. We note that at this point the

Fig. 2 The parameter regions for the existence of critical point A_1. The shaded areas are considered unphysical due to either $\Omega_\phi > 1$ (shaded pink area) or $\Omega_\phi < 0$ (shaded blue area)
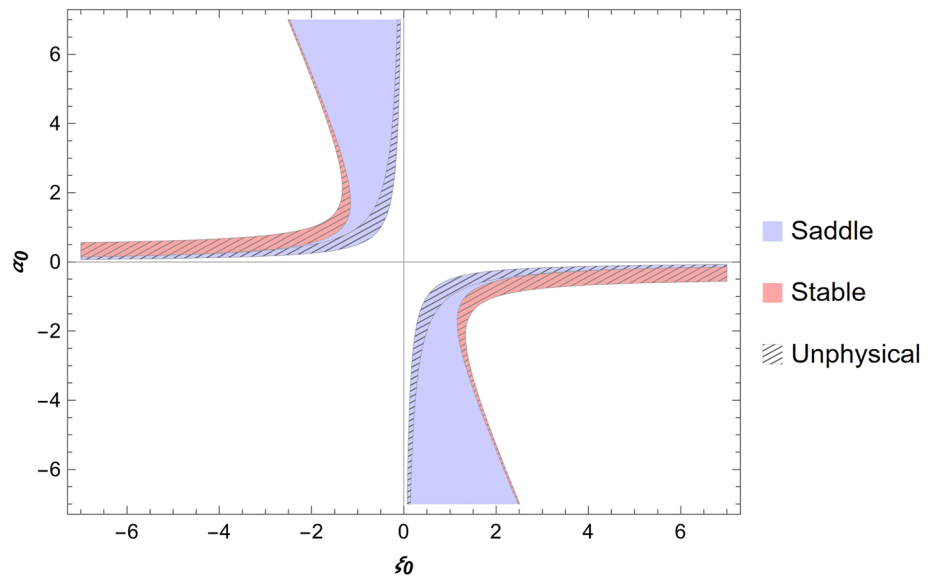
phantom field energy density parameter $\Omega_\phi = 1$, which is invariant under the variation of the parameters α_0 and ξ_0. So, this point represents a phantom field dominated universe and is always physical.

The saddle and physically relevant regions of parameters for A_1 are subsets of the stable regions of A_3, but only under the circumstance that A_1 exists (i.e., the pair of parameters lies in the colored region depicted in Fig. 2). In this scenario, the system will evolve from A_1 to A_3 in the cosmic history since A_2 does not exist for these parameters. However, it is also possible that the parameters do not allow for the existence of A_1 (i.e., they fall outside the colored region depicted in Fig. 2), yet satisfy the physical conditions $0 \leq \Omega_m, \Omega_\phi \leq 1$. Then, A_3 becomes the sole existing critical point and the system will simply converge towards it. The best-fit result of Model vP corresponds to the second scenario.

Figure 5 shows the phase portrait of the viscous phantom field in the late universe. The phase plane is divided into three regions: (i) $\Omega_\phi > 1$ (the light gray region above the upper branch of the blue hyperbola $y^2 - x^2 = 1$); (ii) $0 < \Omega_\phi < 1$ (the region between the upper branch of the blue hyperbola $y^2 - x^2 = 1$ and red straight lines $y = \pm x$); and (iii) $\Omega_\phi < 0$ (the regions below the red straight lines). The blue hyperbola $y^2 - x^2 = 1$ represents all the possible attractors A_3 for different values of parameters $\{\alpha_0, \xi_0\}$. The blue rounded marker indicates the specific attractor point A_3 for the best-fit parameters. The purple hyperbola corresponds to $\Omega_{\phi 0} = 1 - \Omega_{m0} = 0.678$, which is the best-fit density parameter of the phantom field at present time. The green hyperbola corresponds to $\Omega_\phi = 0.018$, which is the value of Ω_ϕ when Ω_m reaches its maximum in the cosmic history, indicating the matter-dominated era calculated from the fitting result.

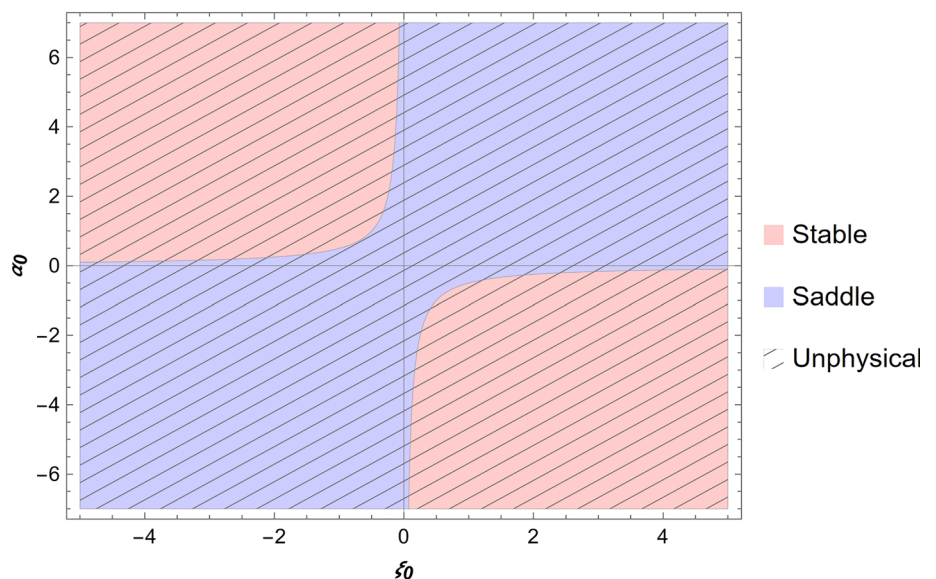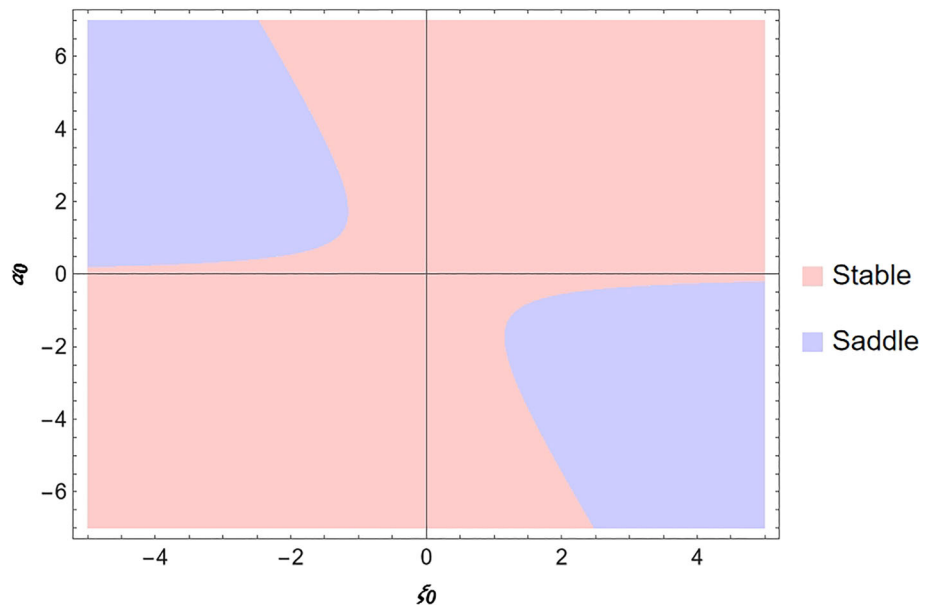**Fig. 3** The parameter regions for the existence of critical point A_2

Fig. 4 The parameter regions for the existence of critical point A_3

Moreover, the total EoS of the cosmic fluid can be expressed in terms of x, y and ζ as

$$w_{\text{tot}} = \frac{p_{\text{eff}} + p_m}{\rho_\phi + \rho_m} = -x^2 - y^2 - \zeta. \tag{18}$$

The universe is in accelerating phase if $-1 < w_{\text{tot}} < -1/3$, and decelerating if $-1/3 < w_{\text{tot}} < 0$. When $w_{\text{tot}} < -1$, the universe will enter the super-acceleration and end in a Big Rig singularity. For Model P which has no viscosity, the region $-1 \le w_{\text{tot}} = -x^2 - y^2 < -1/3$ intercepts with the blue hyperbola $y^2 - x^2 = 1$ only at one point $(x, y) = (0, 1)$, which means that either the model needs severe fine-tuning or it will encounter big rip singularity. This is independent of the fitting. For Model vP, the regions $w_{\text{tot}} \in [-1, -1/3]$ and $w_{\text{tot}} \in [-1/3, 0]$ calculated from the best-fit result are painted cyan and yellow in Fig. 5, respectively. One can see that the cyan region covers a portion of the blue hyperbola

that represents all possibilities of A_3. The best-fit A_3 is in this region. Therefore, the presence of bulk viscosity can indeed allow the model evolve into an attractor that is still in the $w_{\text{tot}} > -1$ region, and help avoid the cosmic singularity.

A heteroclinic orbit representing the evolutionary history of our universe most likely starts somewhere near the green hyperbola (matter dominated era) in the yellow region (decelerating phase with $-1/3 \le w_{\text{tot}} \le 0$), crosses the purple hyperbola (present time) in the cyan region (accelerating phase), and eventually reaches some point on the blue hyperbola (attractor A_3). However, the preceding section of such a heteroclinic orbit seems to cross from the $\Omega_\phi < 0$ region to $\Omega_\phi > 0$ region in early time and encounter a singularity of the phantom field EoS $w_\phi = p_{\text{eff}}/\rho_\phi$. This issue arises because our analysis relies on late time observation data, which do not capture the early stages of cosmic phase transitions. Fur-

Fig. 5 The phase space evolution of the dynamical system for Model vP
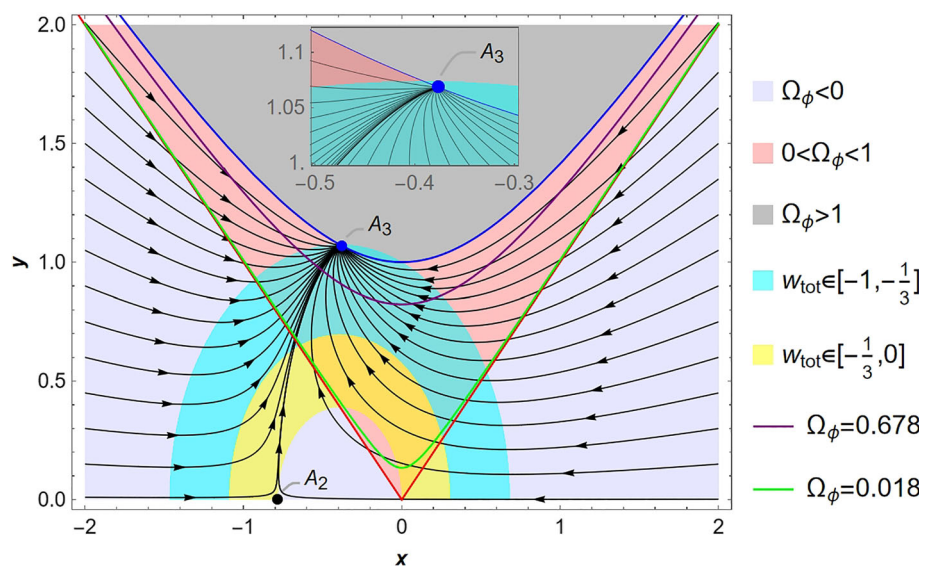
ther research may be needed to address this typical concern rooting from the negative kinetic energy of phantom field.

5 Statefinder diagnostic

The statefinder diagnostic uses the parameters $\{q, r, s\}$ that are derived from higher derivatives of the scale factor,

$$q \equiv -\frac{\ddot{a}}{aH^2}, \quad r \equiv \frac{\dddot{a}}{aH^3}, \quad s \equiv \frac{r-1}{3(q-1/2)}, \quad (19)$$

to differentiate various DE models. For the current model, the parameters are

$$
\begin{aligned}
q &= \frac{1}{2}(1 + 3w_\phi \Omega_\phi), \\
r &= 1 - \frac{3}{2}\frac{\mathrm{d}w_\phi}{\mathrm{d}N}\Omega_\phi + \frac{9}{2}w_\phi(1+w_\phi)\Omega_\phi, \\
s &= 1 - \frac{\mathrm{d}w_\phi}{\mathrm{d}N}\frac{1}{3w_\phi} + w_\phi.
\end{aligned}
\quad (20)
$$

Using the best-fit parameters, we plot the r-q and r-s trajectories for both Model P and Model vP in Figs. 6 and 7, respectively. The present time is indicated by the rounded marker on the curves. As shown in Fig. 6, Model P exhibits a monotonically increasing deviation from the de Sitter point in the future and asymptotes to a point in the region with $q < 0$, $r > 1$. In contrast, Model vP will asymptotically approach a stable fixed point $(q, r) = (-0.9794, 0.9391)$ near the de Sitter point. Figure 7 reveals that both models have $r < 1$ and $s > 0$ in the early universe, and they both cross the ΛCDM point $(0, 1)$, but have different behaviors

afterwards. Model P moves away from the ΛCDM point, while Model vP returns to it and passes it again before converging to a nearby fixed point $(s, r) = (0.0137, 0.9391)$ in the far future.

The effective EoS parameters of the total cosmic fluid, w_{tot}, for both Model P and vP are plotted in Fig. 8. As shown in the figure, w_{tot} of Model vP remains above -1 and asymptotes to -0.9863 in the infinite future, which implies that the universe will avoid the big rip singularity. This result is consistent with the dynamical analysis in the previous section. Moreover, the effective EoS parameter, w_ϕ, of the viscous phantom field is also plotted. One can see that it can cross the phantom divide during the cosmic evolution. In this sense, the phantom field model with viscosity is an effective quintom model. At present time, the effective EoSs of the viscous phantom field and the total cosmic fluid are -1.0565 and -0.7159, respectively.

We also investigate the effect of viscosity on the evolutionary history by computing the ratio K of the effective pressure to the intrinsic pressure of the phantom field, which is defined as

$$K \equiv \frac{p_{eff}}{p_\phi} \sim 1 + \dot{\phi}e^{\frac{\alpha_0}{2}\phi}. \quad (21)$$

Figure 9 shows the evolution of K as a function of $\ln a$. It is evident that viscosity has a significant impact on reducing the pressure of the phantom field, especially around $z = 0.8475$ ($\ln a = -0.6138$), where K reaches a minimum value of about 0.4921 and the pressure of the field is only a half of the intrinsic pressure. At present ($z = 0$), the effective pressure is about one third (32.73%) lower than the intrinsic pressure due

Fig. 6 Evolving trajectories of the statefinder pairs in the q-r plane. The black dot $(-1, 1)$ represents the de Sitter phase, and the solid dots on the lines represent the current state of the models
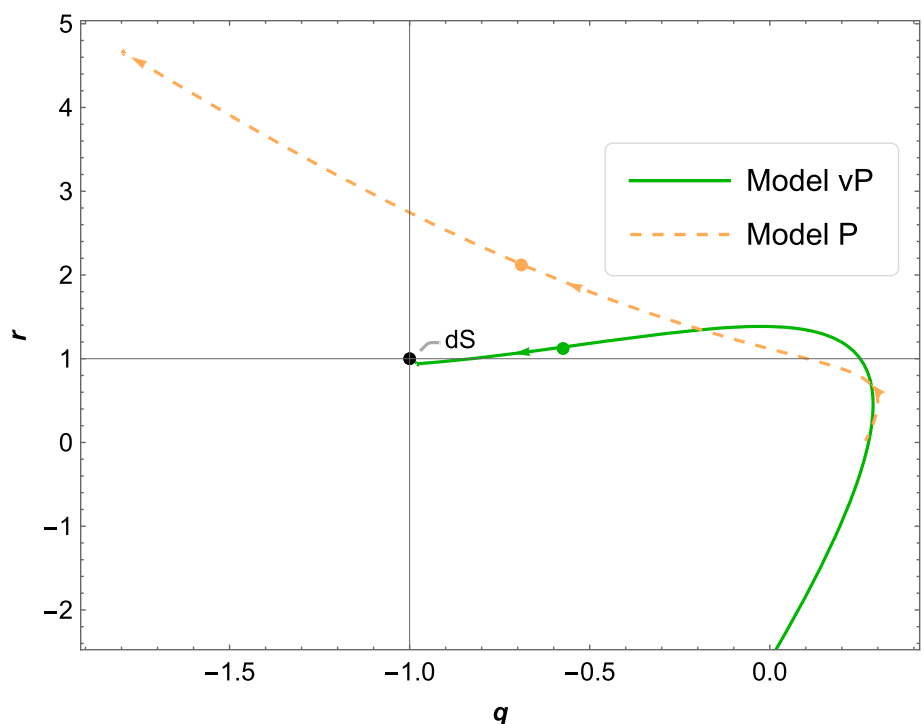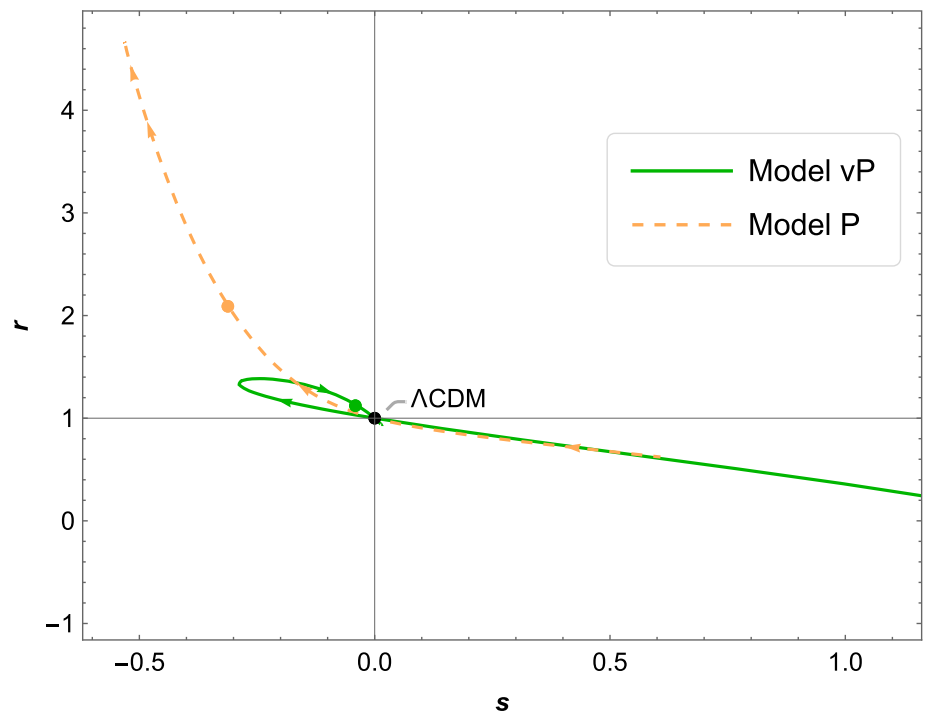
Fig. 7 Evolving trajectories of the statefinder pairs in the *r*-*s* plane. The black dot (0, 1) represents the ΛCDM model, and the solid dots on the lines represent the current state of the models

to viscosity. In the future, viscosity will continue to reduce the intrinsic pressure by about one quarter, as *K* asymptotes to 0.7672.

6 Conclusion and discussions

Recent cosmological observations suggest that the late-time acceleration of the universe is more likely driven by phan-

tom DE rather than quintessence DE. However, phantom DE models typically encounter the big rip singularity problem. In this work, we explore the possibility of avoiding the big rip singularity by introducing bulk viscosity in the phantom field model. We constrain the model parameters using the latest SNIa and H(z) data. The results indicate that the data favor a significant bulk viscosity over a non-constant potential term for the phantom field.

Fig. 8 The evolution of the total EoSs, w_{tot}, of Model P and Model vP, as well as the effective EoS, w_ϕ of Model vP
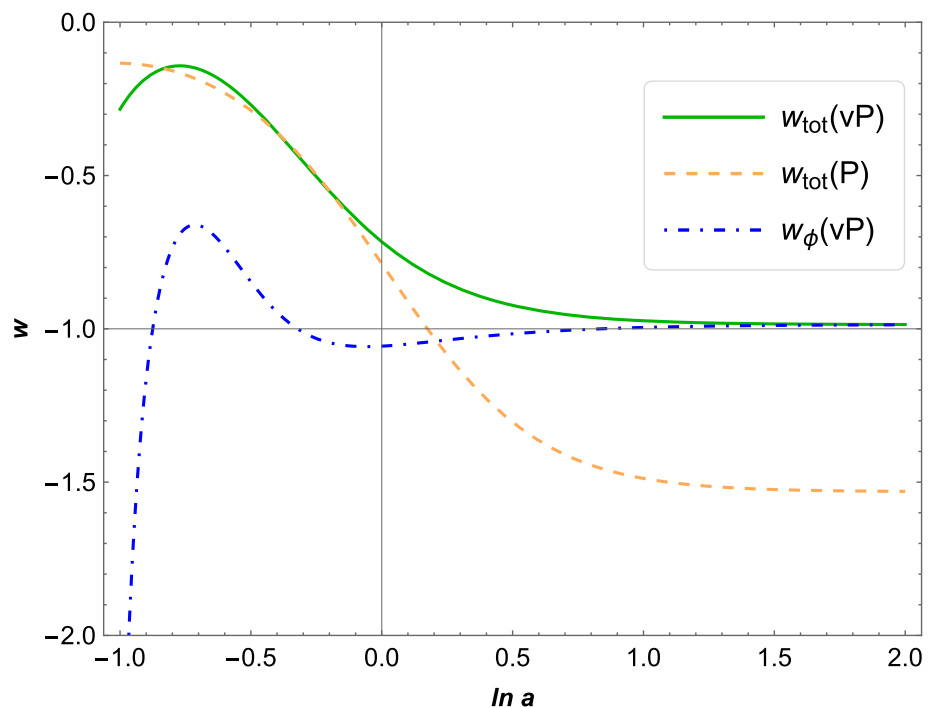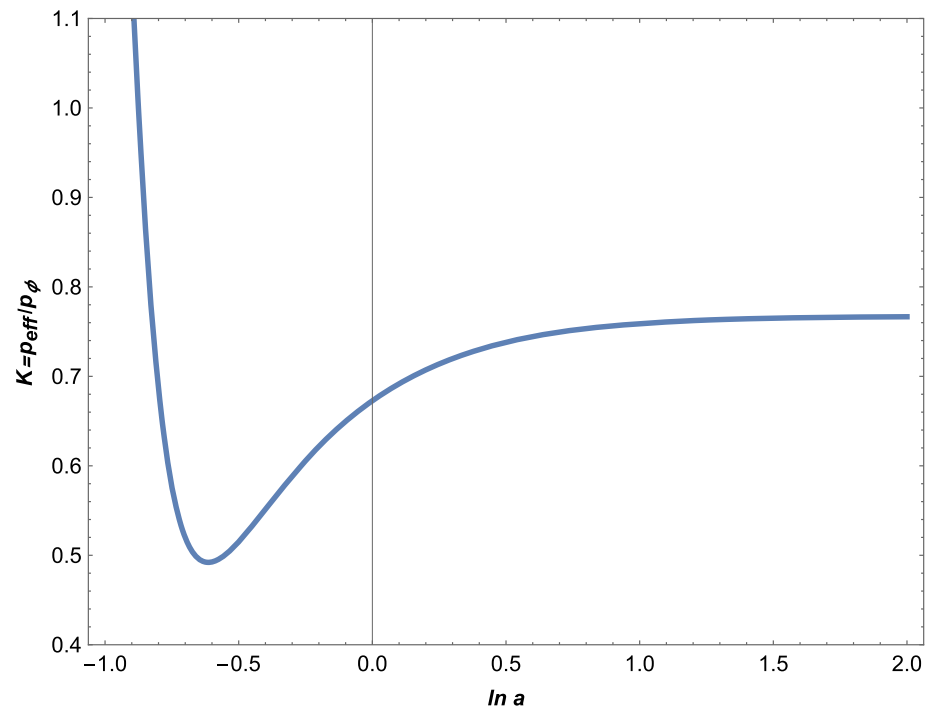
Fig. 9 Evolution of the ratio of effective pressure p_{eff} to scalar field pressure p_ϕ

We then perform a dynamical analysis of the viscous phantom field model using the best-fit values of the parameters. We find that the only stable and physical attractor of the autonomous system is A_3, which corresponds to a phantom-dominated era. The other critical points, may that be either unstable, unphysical, or cannot exist for the best-fit parameters, do not represent different cosmological eras, since the two variables of the autonomous system only correspond to the kinetic and potential energy. We also plot the possible curves that represent the matter-dominated era and the present epoch on the phase portrait. The heteroclinic orbit that describes our universe is expected to cross these curves and converge to the A_3 attractor. However, we cannot trust the early part of the orbit or the critical points that precede the matter-dominated era, since we only fit the model for the late-time behavior. Due to bulk viscosity, some combinations of the parameters may allow the A_3 attractor have a total EoS w_{tot} of cosmic fluid that falls within the accelerating region $-1 < w_{\text{tot}} < -1/3$. This implies that the phantom universe may avoid the big rip singularity and end in a state with $w_{\text{tot}} > -1$ with the presence of bulk viscosity.

We apply the statefinder diagnostic to the viscous phantom field model and compare it with the non-viscous model. We find that the statefinder parameters of the viscous model do not diverge monotonically from the ΛCDM point, but rather approach a nearby fixed point asymptotically. The bulk viscosity acts as a dissipative force that lowers the intrinsic pressure of the phantom field. The viscosity has its maximum effect around $z = 0.8475$, where it lowers the intrinsic pressure by about a half. At the present time ($z = 0$), the viscosity reduces the intrinsic pressure by a third, resulting in a lower effective pressure. In the asymptotic future, the viscosity will still lower the intrinsic pressure by a quarter. This reduction enables the universe to escape the big rip singularity.

For simplicity, we have limited our study to a specific form of the phantom field potential and the bulk viscosity, which may not be the most general or realistic choice. It would be worthwhile to explore other forms of potential and viscosity that can fit the observational data and avoid the big rip singularity. Due to the scope of our work, we have only focused on the late-time behavior of the viscous phantom field model, and ignored the early-time dynamics that may involve other mechanisms. A more comprehensive study should include the full history of the universe and investigate the transitions between different cosmological eras. We also use conventional methods of data analysis and dynamical analysis, which may have some limitations or biases. Future research could employ artificial intelligence techniques to improve the accuracy and efficiency of data fitting, parameter estimation, and model selection [53,54].

Data Availability Statement This manuscript has no associated data or the data will not be deposited. [Authors' comment: Data sharing is not applicable as only public data has been used and no data has been generated.].

References

1. S. Capozziello, M. De Laurentis, Extended theories of gravity. Phys. Rep. **509**, 167 (2011). arXiv:1108.6266 [gr-qc]
2. S. Nojiri, S. Odintsov, V. Oikonomou, modified gravity theories on a nutshell: inflation, bounce and late-time evolution. Phys. Rep. **692**, 1 (2017). arXiv:1705.11098 [gr-qc]
3. S. Weinberg, The cosmological constant problems, in *4th International Symposium on Sources and Detection of Dark Matter in the Universe (DM 2000)* (2000), pp. 18–26. arXiv:astro-ph/0005265
4. S. Bahamonde, C.G. Böhmer, S. Carloni, E.J. Copeland, W. Fang, N. Tamanini, Dynamical systems applied to cosmology: dark energy and modified gravity. Phys. Rep. **775–777**, 1 (2018). arXiv:1712.03107 [gr-qc]
5. D.M. Scolnic et al. [Pan-STARRS1], The complete light-curve sample of spectroscopically confirmed SNe Ia from Pan-STARRS1 and cosmological constraints from the combined pantheon sample. Astrophys. J. **859**, 101 (2018). arXiv:1710.00845 [astro-ph.CO]
6. M. Ishak, Testing general relativity in cosmology. Living Rev. Relativ. **22**, 1 (2019). arXiv:1806.10122 [astro-ph.CO]
7. P.J.E. Peebles, B. Ratra, Cosmology with a time variable cosmological constant. Astrophys. J. Lett. **325**, L17 (1988)
8. B. Ratra, P.J.E. Peebles, Cosmological consequences of a rolling homogeneous scalar field. Phys. Rev. D **37**, 3406 (1988)
9. R.R. Caldwell, A phantom menace? Phys. Lett. B **545**, 23 (2002). arXiv:astro-ph/9908168
10. S.M. Carroll, M. Hoffman, M. Trodden, Can the dark energy equation-of-state parameter w be less than -1? Phys. Rev. D **68**, 023509 (2003). arXiv:astro-ph/0301273
11. N. Aghanim et al. [Planck], Planck 2018 results. VI. Cosmological parameters. Astron. Astrophys. **641**, A6 (2020) [Erratum: Astron. Astrophys. 652, C4 (2021)]. arXiv:1807.06209 [astro-ph.CO]
12. J. Beltran Jimenez, R. Lazkoz, D. Saez-Gomez, V. Salzano, Observational constraints on cosmological future singularities. Eur. Phys. J. C **76**, 631 (2016). arXiv:1602.06211 [gr-qc]
13. R.R. Caldwell, M. Kamionkowski, N.N. Weinberg, Phantom energy and cosmic doomsday. Phys. Rev. Lett. **91**, 071301 (2003). arXiv:astro-ph/0302506
14. V. Sahni, A. Shafieloo, A.A. Starobinsky, Model independent evidence for dark energy evolution from Baryon Acoustic Oscillations. Astrophys. J. Lett. **793**, L40 (2014). arXiv:1406.2209 [astro-ph.CO]
15. V. Sahni, Dark matter and dark energy. Lect. Notes Phys. **653**, 141 (2004). arXiv:astro-ph/0403324
16. M. Sami, A. Toporensky, Phantom field and the fate of universe. Mod. Phys. Lett. A **19**, 1509 (2004). arXiv:gr-qc/0312009
17. Z.-K. Guo, R.-G. Cai, Y.-Z. Zhang, Cosmological evolution of interacting phantom energy with dark matter. JCAP **05**, 002. arXiv:astro-ph/0412624
18. Z.-K. Guo, Y.-Z. Zhang, Interacting phantom energy. Phys. Rev. D **71**, 023501 (2005). arXiv:astro-ph/0411524
19. S. Nojiri, S.D. Odintsov, S. Tsujikawa, Properties of singularities in (phantom) dark energy universe. Phys. Rev. D **71**, 063004 (2005). arXiv:hep-th/0501025
20. B.-R. Chang, H.-Y. Liu, L.-X. Xu, C.-W. Zhang, Y.-L. Ping, Statefinder parameters for interacting phantom energy with dark matter. JCAP **01**, 016. arXiv:astro-ph/0612616
21. R. Curbelo, T. Gonzalez, G. Leon, I. Quiros, Interacting phantom energy and avoidance of the big rip singularity. Class. Quantum Gravity **23**, 1585 (2006). arXiv:astro-ph/0502141
22. M.R. Setare, Interacting holographic phantom. Eur. Phys. J. C **50**, 991 (2007). arXiv:hep-th/0701085
23. X. Fu, H.W. Yu, P. Wu, Dynamics of interacting phantom scalar field dark energy in Loop Quantum Cosmology. Phys. Rev. D **78**, 063001 (2008). arXiv:0808.1382 [gr-qc]
24. J. de Haro, J. Amoros, E. Elizalde, On the fate of the phantom dark energy universe in semiclassical gravity II: scalar phantom fields. Phys. Rev. D **86**, 083528 (2012). arXiv:1206.6948 [gr-qc]
25. H. Amirhashchi, Phantom instability of viscous dark energy in anisotropic space-time. Astrophys. Space Sci. **345**, 439 (2013). arXiv:1304.2292 [astro-ph.CO]
26. M. Sami, P. Singh, S. Tsujikawa, Avoidance of future singularities in loop quantum cosmology. Phys. Rev. D **74**, 043514 (2006). arXiv:gr-qc/0605113
27. T. Koivisto, D.F. Mota, Cosmology and astrophysical constraints of Gauss–Bonnet dark energy. Phys. Lett. B **644**, 104 (2007). arXiv:astro-ph/0606078
28. S. Nojiri, S.D. Odintsov, The future evolution and finite-time singularities in F(R)-gravity unifying the inflation and cosmic acceleration. Phys. Rev. D **78**, 046006 (2008). arXiv:0804.3519 [hep-th]
29. G. Huey, B.D. Wandelt, Interacting quintessence. The Coincidence problem and cosmic acceleration. Phys. Rev. D **74**, 023519 (2006). arXiv:astro-ph/0407196
30. H. Wei, R.-G. Cai, Interacting agegraphic dark energy. Eur. Phys. J. C **59**, 99 (2009). arXiv:0707.4052 [hep-th]
31. H. Okumura, F. Yonezawa, New expression of the bulk viscosity. Physica A Stat. Mech. Appl. **321**, 207 (2003). (**statphys-Taiwan-2002: Lattice Models and Complex Systems**)
32. M.M. Disconzi, T.W. Kephart, R.J. Scherrer, New approach to cosmological bulk viscosity. Phys. Rev. D **91**, 043532 (2015). arXiv:1409.4918 [gr-qc]
33. I. Brevik, O. Grøn, J. de Haro, S.D. Odintsov, E.N. Saridakis, Viscous cosmology for early- and late-time universe. Int. J. Mod. Phys. D **26**, 1730024 (2017). arXiv:1706.02543 [gr-qc]
34. M. Cataldo, N. Cruz, S. Lepe, Viscous dark energy and phantom evolution. Phys. Lett. B **619**, 5 (2005). arXiv:hep-th/0506153
35. I. Brevik, E. Elizalde, S. Nojiri, S.D. Odintsov, Viscous little rip cosmology. Phys. Rev. D **84**, 103508 (2011)
36. L. Sebastiani, Finite-time singularities in modified F(R, G)-gravity and singularity avoidance. Springer Proc. Phys. **137**, 261 (2011). arXiv:1008.3041 [gr-qc]
37. X.-H. Meng, Z.-Y. Ma, Rip/singularity free cosmology models with bulk viscosity. Eur. Phys. J. C **72**, 2053 (2012). arXiv:1202.4936 [astro-ph.CO]
38. I. Brevik, Viscosity-induced crossing of the phantom barrier. Entropy **17**, 6318 (2015). arXiv:1509.03489 [gr-qc]
39. R.D. Boko, M.J.S. Houndjo, Cosmological viscous fluid models describing infinite time singularities in f(T) gravity. Eur. Phys. J. C **80**, 855 (2020)
40. C.P. Singh, S. Kaur, Probing bulk viscous matter-dominated model in Brans–Dicke theory. Astrophys. Space Sci. **365**, 2 (2020)
41. N. Cruz, E. González, J. Jovel, Singularities and soft-Big Bang in a viscous ΛCDM model. Phys. Rev. D **105**, 024047 (2022). arXiv:2109.09865 [gr-qc]
42. E.J. Copeland, A.R. Liddle, D. Wands, Exponential potentials and cosmological scaling solutions. Phys. Rev. D **57**, 4686 (1998). arXiv:gr-qc/9711068
43. S.C.C. Ng, N.J. Nunes, F. Rosati, Applications of scalar attractor solutions to cosmology. Phys. Rev. D **64**, 083510 (2001). arXiv:astro-ph/0107321

44. J.-G. Hao, X.-Z. Li, An Attractor solution of phantom field. Phys. Rev. D **67**, 107303 (2003). arXiv:gr-qc/0302100
45. J.-G. Hao, X.-Z. Li, Phantom cosmic dynamics: tracking attractor and cosmic doomsday. Phys. Rev. D **70**, 043529 (2004). arXiv:astro-ph/0309746
46. X.-Z. Li, J.-G. Hao, Phantom field with o(n) symmetry in an exponential potential. Phys. Rev. D **69**, 107303 (2004). arXiv:hep-th/0303093
47. X.-Z. Li, Y.-B. Zhao, C.-B. Sun, Heteroclinic orbit and tracking attractor in cosmological model with a double exponential potential. Class. Quantum Gravity **22**, 3759 (2005). arXiv:astro-ph/0508019
48. G.S. Sharov, V.O. Vasiliev, How predictions of cosmological models depend on Hubble parameter data sets. Math. Model. Geom. **6**, 1 (2018). arXiv:1807.07323 [gr-qc]
49. J. Yang, R.-H. Lin, X.-H. Zhai, Viscous cosmology in f(T) gravity. Eur. Phys. J. C **82**, 1039 (2022). arXiv:2208.09991 [gr-qc]
50. J. Yang, X.-Y. Fan, C.-J. Feng, X.-H. Zhai, Latest data constraint of some parameterized dark energy models. Chin. Phys. Lett. **40**, 019801 (2023). arXiv:2211.15881 [astro-ph.CO]
51. P.J. Steinhardt, L.-M. Wang, I. Zlatev, Cosmological tracking solutions. Phys. Rev. D **59**, 123504 (1999). arXiv:astro-ph/9812313
52. L.A. Urena-Lopez, Scalar phantom energy as a cosmological dynamical system. JCAP **09**, 013. arXiv:astro-ph/0507350
53. Q.-B. Cheng, C.-J. Feng, X.-H. Zhai, X.-Z. Li, Artificial neural network for constructing type Ia supernovae spectrum evolution model. Phys. Rev. D **97**, 123530 (2018). arXiv:1801.01723 [astro-ph.CO]
54. S. Vagnozzi, S. Dhawan, M. Gerbino, K. Freese, A. Goobar, O. Mena, Constraints on the sum of the neutrino masses in dynamical dark energy models with $w(z) \geq -1$ are tighter than those obtained in ΛCDM. Phys. Rev. D **98**, 083501 (2018). arXiv:1801.08553 [astro-ph.CO]